

Distribution and Dynamics of Hydrogen in the Low-Temperature Phase of Mg₂NiH₄ Studied by Solid-State NMR

Shigenobu Hayashi*

Institute for Materials & Chemical Process, National Institute of Advanced Industrial Science and Technology (AIST), Tsukuba Central 5, 1-1-1 Higashi, Tsukuba, Ibaraki 305-8565, Japan

Received June 18, 2001

Distribution and dynamics of hydrogen atoms in the low-temperature phase of Mg₂NiH₄ have been studied by means of ²H and ¹H NMR for Mg₂NiD₄ and Mg₂NiH₄, respectively. ²H NMR spectra have been measured in the temperature range between 200 and 340 K, and the line shapes were simulated. The temperature dependence of ²H NMR spectra was quite well simulated assuming a distorted tetrahedral configuration and a pseudoisotropic rotation of the NiD₄ unit. The estimated jump frequency obeyed Arrhenius relation with a frequency factor of $(0.8 \pm 0.6) \times 10^{13}$ Hz and an activation energy of 50.1 ± 1.4 kJ/mol. ¹H NMR spectra were acquired from 240 to 360 K. The observed ¹H second moments were 202 kHz² in the rigid lattice (240 K) and 46.6 kHz² in a motional state (360 K). The value in the rigid lattice supported the tetrahedron model, and the value in a motional state indicated the isotropic rotation of the NiH₄ unit. Conclusively, the NiH₄ unit has the distorted tetrahedral configuration and undergoes the pseudoisotropic rotation.

Introduction

Metal hydrides are attractive for hydrogen storage materials. Magnesium–nickel alloy has become one of the promising materials because of its large hydrogen capacity per weight, ever since Reilly and Wiswall found that the alloy reacts readily with hydrogen to form a stable hydride, Mg₂NiH₄.¹ The hydride shows a phase transition of the crystal structure at about 500 K.² In the high-temperature phase, metal atoms form a cubic CaF₂-type structure. Schefer et al.³ and Yvon et al.⁴ concluded from their neutron diffraction results that hydrogen atoms distribute over the six sites which are located at the corners of the octahedrons centered on nickel atoms, although the local configuration of the hydrogen atoms around the nickel atom could not be determined. Noréus and Olsson reported the localized character of the motion of the hydrogen atoms by a cold neutron scattering experiment and proposed a model in which a square planar unit of four hydrogen atoms randomly flips around the nickel atom.⁵

In the low-temperature phase, on the other hand, the metal atoms form a slightly distorted structure of the above high-temperature phase.^{6–9} The metal lattice symmetry was established, while the local configuration of the hydrogen atoms around the nickel atom was argued up to very recent years. Noréus and Werner proposed an octahedron model in which four hydrogen atoms form a square plane centered on a nickel atom,¹⁰ as illustrated in Figure 1a. On the other hand, Zolliker et al. proposed a tetrahedron model (Figure 1b), where four hydrogen atoms occupy the four corners of the tetrahedron centered on a nickel atom.¹¹ Crystal structure studies of related compounds such as Mg₂FeH₆ and Mg₂CoH₅ supported the tetrahedron model in Mg₂NiH₄.^{12,13} Quantum chemical calculation resulted in a conclusion that a [NiH₄]²⁻ complex had a square planar structure while a

* E-mail: hayashi.s@aist.go.jp. Fax: +81-298-61-4515.

- (1) Reilly, J. J.; Wiswall, R. H., Jr. *Inorg. Chem.* **1968**, *7*, 2254–2256.
- (2) Gavra, Z.; Mintz, M. H.; Kimmel, G.; Hadari, Z. *Inorg. Chem.* **1979**, *18*, 3595–3597.
- (3) Schefer, J.; Fisher, P.; Hälgl, W.; Stucki, F.; Schlapbach, L.; Didisheim, J. J.; Yvon, K.; Andresen, A. F. *J. Less-Common Met.* **1980**, *74*, 65–73.
- (4) Yvon, K.; Schefer, J.; Stucki, F. *Inorg. Chem.* **1981**, *20*, 2776–2778.

- (5) Noréus, D.; Olsson, L. G. *J. Chem. Phys.* **1983**, *78*, 2419–2427.
- (6) Noréus, D.; Werner, P.-E. *Mater. Res. Bull.* **1981**, *16*, 199–206.
- (7) Ono, S.; Hayakawa, H.; Suzuki, A.; Nomura, K.; Nishimiya, N.; Tabata, T. *J. Less-Common Met.* **1982**, *88*, 63–71.
- (8) Hayakawa, H.; Ishido, Y.; Nomura, K.; Uruno, H.; Ono, S. *J. Less-Common Met.* **1984**, *103*, 277–283.
- (9) Zolliker, P.; Yvon, K.; Baerlocher, C. *J. Less-Common Met.* **1986**, *115*, 65–78.
- (10) Noréus, D.; Werner, P.-E. *J. Less-Common Met.* **1984**, *97*, 215–222.
- (11) Zolliker, P.; Yvon, K.; Jorgensen, J. D.; Rotella, F. J. *Inorg. Chem.* **1986**, *25*, 3590–3593.
- (12) Didisheim, J.-J.; Zolliker, P.; Yvon, K.; Fischer, P.; Schefer, J.; Gubelmann, M.; Williams, A. F. *Inorg. Chem.* **1984**, *23*, 1953–1957.
- (13) Zolliker, P.; Yvon, K.; Fischer, P.; Schefer, J. *Inorg. Chem.* **1985**, *24*, 4177–4180.

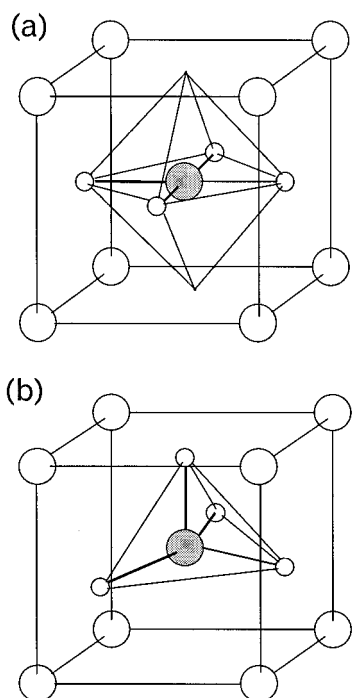


Figure 1. Models of the configuration of hydrogen atoms around a Ni atom: (a) the octahedron model with a square-planar NiH₄ unit and (b) the tetrahedron model.

[NiH₄]⁴⁻ complex led to a tetrahedral structure.¹⁴ A recent ab initio calculation suggested a tetrahedrally distorted square-planar configuration around the nickel atom forming [NiH₄]⁴⁻.¹⁵

NMR is a powerful tool to study hydrogen motions in materials. In previous papers,^{16,17} we have studied the motion of the hydrogen atoms in the low- and high-temperature phases of Mg₂NiH₄ by means of ¹H NMR. We concluded that the motion of the hydrogen atoms is localized in the low-temperature phase. The ¹H NMR results supported the square planar model rather than the tetrahedron model.¹⁸ Ueda et al. have tried to identify the configuration by means of ²H NMR using a deuteride, Mg₂NiD₄.¹⁹ The results supported the tetrahedron model, but the dynamics was not concluded because of its complicated nature. Consequently, the previous ¹H and ²H NMR results were inconsistent with each other.

In the present work, the local configuration and dynamics of hydrogen atoms in the low-temperature phase of Mg₂NiH₄ have been studied by means of ²H and ¹H NMR for Mg₂NiD₄ and Mg₂NiH₄, respectively. We conclude that a distorted tetrahedral configuration explains both the ²H and ¹H NMR results. Simulation of the ²H NMR spectra reveals the dynamics of deuterium atoms, which is a pseudoisotropic

rotation of the NiH₄ unit. The estimated jump frequency is in excellent agreement with the previous ¹H NMR results.¹⁶

Experimental Section

Materials. The samples of Mg₂NiH₄ and Mg₂NiD₄ were synthesized by the reaction between stoichiometric Mg₂Ni and protium/deuterium gas. The Mg₂NiH₄ sample was the same as that previously used.^{16,17} The Mg₂NiD₄ sample was synthesized in conditions similar to those for Mg₂NiH₄ and used also in the previous work.¹⁹

²H and ¹H NMR Measurements. ²H NMR spectra were measured by a Bruker MSL400 spectrometer with a static magnetic field of 9.4 T. ²H Larmor frequency was 61.42 MHz. The quadrupole echo pulse sequence (90°_x-τ₁-90°_y-τ₂-echo) was used, and the latter half of the echo signal was acquired and Fourier transformed. The 90° pulse width was 2.6 μs, the pulse interval τ₁ between two 90° pulses was 15 μs, and the repetition time was between 10 and 60 s. The τ₂ value was adjusted to the echo maximum in the data processing. The sample temperature was varied from 200 to 340 K.

¹H NMR spectra were measured by a Bruker ASX200 spectrometer with a field of 4.7 T. ¹H Larmor frequency was 200.13 MHz. The solid echo pulse sequence was used, which is the same as the quadrupole echo sequence. The 90° pulse width was 1.15 μs, the pulse interval was 10 μs, and the repetition time was between 30 and 300 s. The sample temperature was varied between 240 and 360 K.

²H spectra composed of staticlike powder patterns, and ¹H spectra were simulated by our own software written in Fortran and running on an NEC PC-9801 series computer. The ²H spectra whose line shapes were modulated by motions were simulated using MXET1 program²⁰ installed on an IBM SP2 computer system.

Results and Discussion

²H NMR Spectra. A ²H spin has a quadrupole moment with a spin quantum number *I* of 1. The quadrupole coupling constant is of the order of 100 kHz, and then, ²H NMR spectra are sensitive to motions with a frequency of about 100 kHz. Figure 2 shows temperature dependence of ²H NMR spectra in Mg₂NiD₄. Some similar spectra have already been reported without any discussions.²¹ The line shape shows negligible changes below 260 K. The central peak starts to grow up at 260 K. A drastic change is observed between 280 and 330 K. Above 330 K, one relatively sharp line is observed with tails at the bottom on both sides. The tailing part becomes smaller with increase in temperature.

These results indicate that ²H spins are in a rigid lattice state below 260 K. The spectrum at 200 K is deconvoluted into four components with equal populations, using static powder line shapes, as shown in Figure 3. This means that there are at least four crystallographically inequivalent sites. The peaks and shoulders in the spectra are observed reproducibly between 200 and 260 K, although the signal-to-noise ratio seems to be fairly poor. Figure 3 shows the only fit which we obtained. The obtained quadrupole parameters, quadrupole coupling constants (QCC = *e*²*Qq*/*h*) and

(14) Lindberg, P.; Noréus, D.; Blomberg, M. R. A.; Siegbahn, P. E. M. *J. Chem. Phys.* **1986**, *85*, 4530–4537.

(15) García, G. N.; Abriata, J. P.; Sofo, J. O. *Phys. Rev. B* **1999**, *59*, 11746–11754.

(16) Hayashi, S.; Hayamizu, K.; Yamamoto, O. *J. Chem. Phys.* **1983**, *79*, 2308–2314.

(17) Hayashi, S.; Hayamizu, K.; Yamamoto, O. *J. Chem. Phys.* **1983**, *79*, 5572–5578.

(18) Hayashi, S.; Hayamizu, K. *J. Less-Common Met.* **1989**, *155*, 31–35.

(19) T. Ueda, S. Hayashi, K. Hayamizu, E. Akiba, Japanese Conference on Molecular Structures, Kyoto, 1992.

(20) Greenfield, M. S.; Ronemus, A. D.; Vold, R. L.; Vold, R. R.; Ellis, P. D.; Raidy, T. E. *J. Magn. Reson.* **1987**, *72*, 89–107.

(21) Hayashi, S.; Orimo, S.; Fujii, H. *J. Alloys Compd.* **1997**, *261*, 145–149.

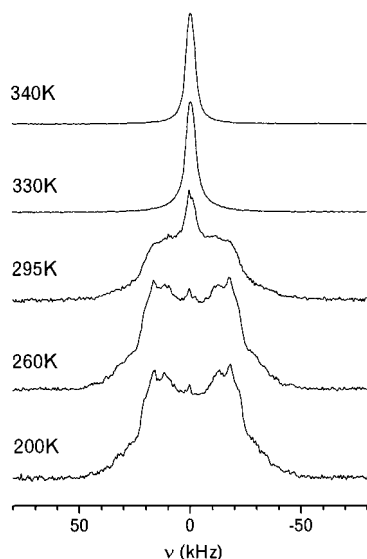


Figure 2. Temperature dependence of ^2H NMR spectra of Mg_2NiD_4 .

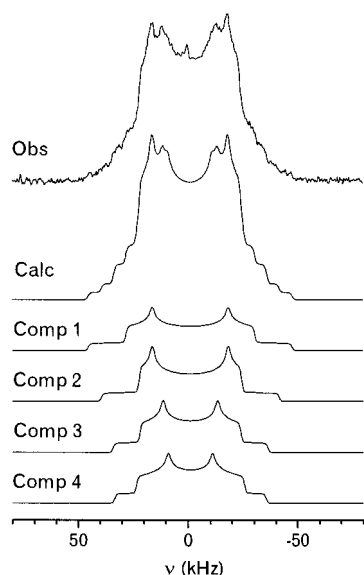


Figure 3. ^2H NMR spectra at 200 K and its deconvoluted results.

asymmetry factors (η_Q), are 62 kHz and 0.26 for site 1, 54 kHz and 0.15 for site 2, 47 kHz and 0.30 for site 3, and 46 kHz and 0.42 for site 4, respectively. Experimental errors are ± 2 kHz and ± 0.04 for QCC and η_Q , respectively. The line shapes do not appear to contain an additional anisotropic contribution from the Knight shift, indicating that Mg_2NiD_4 is nonmetallic. This is consistent with the results of ^1H spin–lattice relaxation time T_1 ,¹⁶ which has no effect of conduction electrons. The quadrupole coupling constant is much smaller than those in the C–D and O–D bonds of typical organic compounds (about 200 kHz).

The line shapes modulated by motions are simulated assuming local configurations and motional models. Because the previous ^1H NMR results revealed single activation energy over the wide temperature range 210–450 K, a single mode of motion is assumed rather than a combination of more than one mode. First, the tetrahedral configuration is assumed. If the tetrahedron rotates around a specific axis, the line shape at the fast motional limit should have a pattern

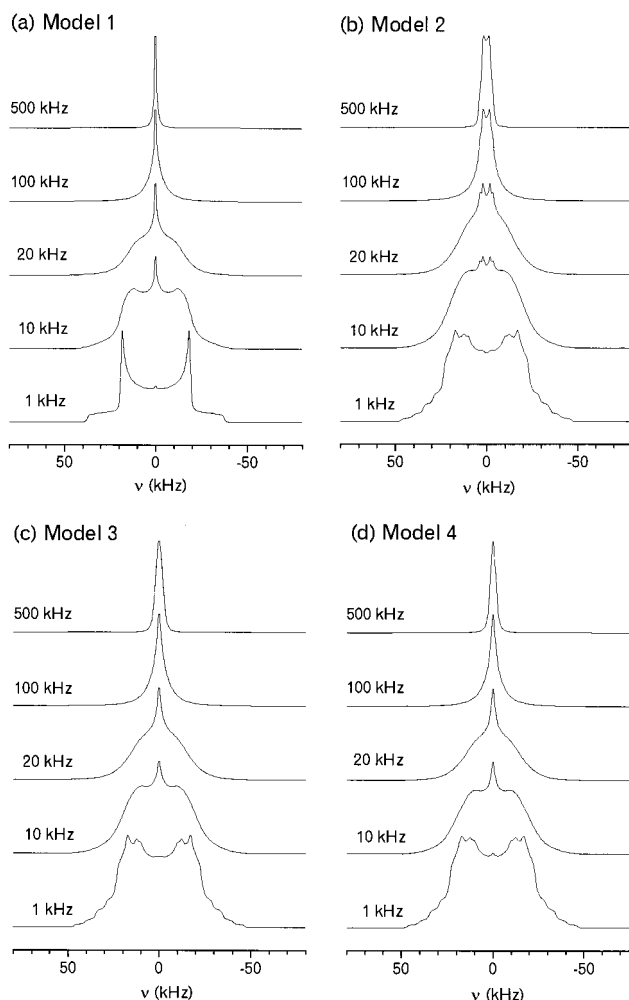


Figure 4. Calculated ^2H NMR spectra assuming the motion described in the text: (a) model 1, (b) model 2, (c) model 3, and (d) model 4. The numbers in the figure are the jump frequency from one site to another site.

Table 1. Euler Angles in Wigner Rotation Used for the Simulations

| site | models 1 & 2 | | | model 3 | | | model 4 | | |
|------|--------------|------------|------------|--------------|------------|------------|--------------|------------|------------|
| | θ [°] | ϕ [°] | ψ [°] | θ [°] | ϕ [°] | ψ [°] | θ [°] | ϕ [°] | ψ [°] |
| 1 | 54.7 | 135 | 0 | 54.7 | 135 | 90 | 58.7 | 135 | 0 |
| 2 | 125.3 | 225 | 0 | 125.3 | 225 | 0 | 121.3 | 225 | 0 |
| 3 | 54.7 | 315 | 0 | 54.7 | 315 | 90 | 58.7 | 315 | 0 |
| 4 | 125.3 | 45 | 0 | 125.3 | 45 | 0 | 121.3 | 45 | 0 |

characteristic of quadrupole interaction. Because the observed spectra show a single narrow line at the higher temperatures, isotropic (or pseudoisotropic) rotation of the tetrahedron is assumed. Figure 4 shows some typical results of the spectrum simulation. Table 1 lists angular parameters used for the simulations, which specify the locations of deuterium in the tetrahedron centered on a nickel atom. The principal axis system (PAS) of the quadrupole interaction is converted to the Zeeman axis system (ZAS) (i.e., the crystal lattice system) by Wigner rotation of the coordinate system; rotation around the z axis by the angle ψ , rotation around the new y axis by the angle θ , and then rotation around the new z axis by the angle ϕ . The direction from Ni to D is assumed to be parallel to the z axis of the PAS, because the presence of Ni–D bonds is reasonably presumed. The z axis of the ZAS is fixed to the C_2 axis of the tetrahedron.

In model 1, the local configuration of hydrogen atoms is assumed to be a regular tetrahedron with four equivalent sites ($\text{QCC} = 50 \text{ kHz}$ and $\eta_Q = 0$). The observed trend is reproduced fairly well at the intermediate and high temperature ranges, as shown in Figure 4a. Actually, there are four inequivalent sites. In model 2, the quadrupole parameters obtained experimentally are used with the regular tetrahedron configuration. The calculated spectra shown in Figure 4b show always split peaks in the central part, being inconsistent with the observed spectra. To avoid the central peak splitting the angles, ψ values are varied in model 3, keeping the regular tetrahedral configuration with the four inequivalent sites. There are several combinations of ψ values with no peak splitting, as shown in Figure 4c. At the higher temperature range, the line width increases gradually, and the central peak splits at the fast motional limit. According to the crystal structure studies,¹¹ the NiH_4 tetrahedron is distorted. In model 4, the configuration is a distorted tetrahedron with the four inequivalent sites. The angles θ are varied, and the best fitting is obtained at $\theta = 54.7 + 4^\circ$, as shown in Figure 4d. The line shapes are almost the same as those in model 3 without the central peak splitting at the fast limit.

Spectrum simulations were carried out also assuming configurations other than the tetrahedron. The results are briefly summarized later without presenting the calculated spectra. If the NiD_4 unit is square planar and the plane rotates around an axis perpendicular to the plane, a Pake doublet pattern with $\eta_Q = 0$ should be observed at the fast limit. Next, hydrogen atoms are assumed to occupy four of the six sites at the corners of an octahedron centered on a Ni atom. The NiD_4 unit might form a square plane, and the plane is assumed to undergo an isotropic rotation. The calculated spectra have extra peaks at the intermediate temperature range and, furthermore, this motion needs six sites. Consequently, the configurations other than the tetrahedron are prohibited.

In conclusion, model 4 is the best among the models. There might be a combined model of models 3 and 4. However, further improvement is impossible and has no significance. Therefore, the experimental line shapes are simulated using model 4 in detail in order to derive the jump frequency. Figure 5 shows some simulated spectra as well as the observed ones. The fine structures remain in the observed spectra at the higher temperature than in the simulated spectra. This discrepancy might come from a distribution of the jump frequency.

Figure 6 shows an Arrhenius plot of the jump frequency, which results in a frequency factor of $(0.8 \pm 0.6) \times 10^{13} \text{ Hz}$ and an activation energy of $50.1 \pm 1.4 \text{ kJ/mol}$. In our previous work,¹⁶ the jump frequency was obtained from ^1H NMR results. The values obtained from the ^1H spin–lattice relaxation time in the rotating frame, $T_{1\rho}$, are also plotted in Figure 6, from which a frequency factor of $2.2 \times 10^{13} \text{ Hz}$ and an activation energy of 51.9 kJ/mol were obtained. Those values are in excellent agreement with the present results.

Roughly speaking, the frequency factor corresponds to a local vibrational frequency of H atoms. Noréus and Olsson observed the optical mode of the vibration centered at 100 meV ($=2.4 \times 10^{13} \text{ Hz}$) in the low-temperature phase of

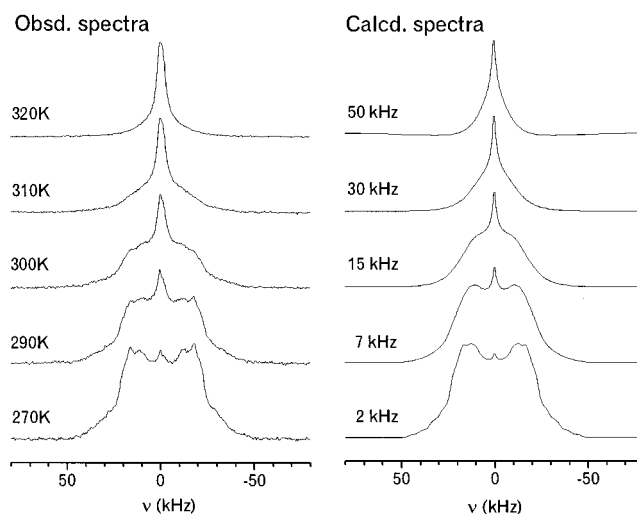


Figure 5. ^2H NMR spectra observed (left) and their simulated spectra (right). The numbers in the figure are the sample temperature and the jump frequency.

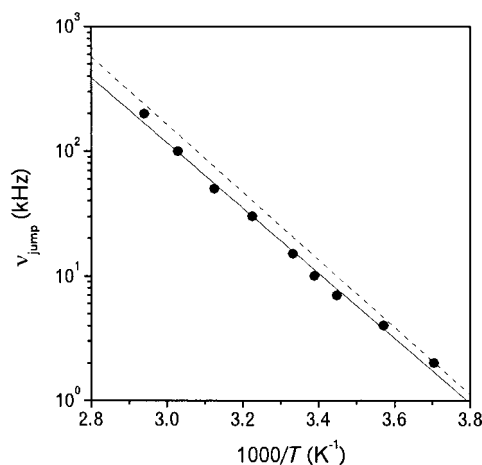


Figure 6. Arrhenius plot of the jump frequency. The solid line is the least-squares fit, while the chain line indicates the results obtained from ^1H $T_{1\rho}$.¹⁶

Mg_2NiH_4 by means of inelastic neutron scattering.⁵ The vibrational frequency agrees very well with the previously described frequency factors.

^1H NMR Spectra. The second moment, M_2 , of a ^1H NMR signal provides good information on the hydrogen distribution and the mode of the hydrogen motion. The previous results could not be explained by the tetrahedral configuration.¹⁸ In the previous works, we reported that the second moment in the rigid lattice was 308 kHz^2 (17 Oe^2) while it was $60 \pm 4 \text{ kHz}^2$ ($3.3 \pm 0.2 \text{ Oe}^2$) between 340 and 500 K.^{16,17} The value in the rigid lattice was too large to be explained by the tetrahedral configuration. The value of 60 kHz^2 was not satisfactorily explained by a single mode of motion. Even if the tetrahedral arrangement is distorted, those are not explained. Then, in the present work, the spectra were remeasured with a spectrometer which had a short 90° pulse width and a short recovery time.

The line narrowing takes place between 270 and 340 K.¹⁶ The line widths are constant below 270 and above 340 K. Hydrogen atoms are in a rigid lattice state below 270 K, while they undergo a localized motion above 340 K. Figure

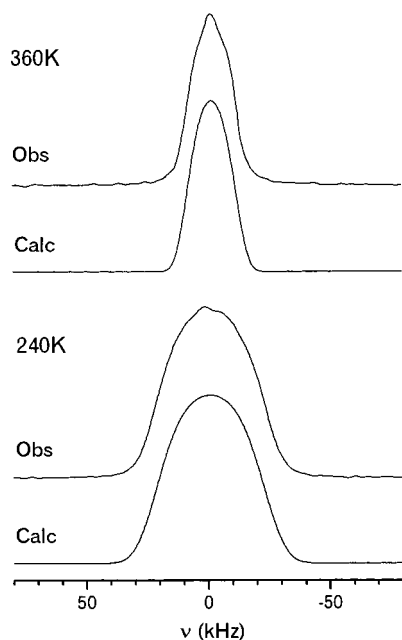


Figure 7. ^1H NMR spectra and their simulated line shapes.

7 shows ^1H spectra at 240 and 360 K. The line shapes are fitted by a rectangular Gaussian line shape proposed by Powles and Carazza²² and expressed as

$$f(x) = h \exp\left(-\frac{x^2}{a^2} - \frac{x^4}{b^4}\right) \quad (1)$$

where h , a , and b are parameters defining the line shape. The parameters obtained from the fitting are $a = 36.6$ kHz and $b = 27.1$ kHz at 240 K and $a = 14.1$ kHz and $b = 14.1$ kHz at 360 K. The second and the fourth moments are estimated numerically from the fitted rectangular Gaussian line shapes. The second moments, M_2 , are 202 and 46.6 kHz² at 240 and 360 K, respectively. The roots of the fourth moment, $M_4^{1/2}$, are 308 and 72.7 kHz² at 240 and 360 K, respectively. If the line shape is Gaussian, the $M_4/(M_2)^2$ value is 3. The obtained ratios are 2.32 and 2.43 at 240 and 360 K, respectively. The present second moments are much smaller than the previous ones (308 and 60 kHz²). In the previous works, the line shapes were distorted, probably because the 90° pulse width and the recovery time were not short enough.

Only the ^1H spins should be taken into consideration in Mg_2NiH_4 , because Mg and Ni nuclei can be neglected in view of the magnetic dipole moment. In the rigid lattice state, the second moment, M_2 , can be expressed as follows:²³

$$M_2 = \frac{3}{5} \gamma_I^4 \hbar^2 I(I+1) \sum_i \frac{1}{r_i^6} \quad (2)$$

where γ_I is the gyromagnetic ratio, \hbar Planck's constant, I the spin quantum number, and r_i the distance between

(22) Powles, J. G.; Carazza, B. *J. Phys. A: Gen. Phys.* **1970**, *3*, 335–341.

(23) Abragam, A. *The Principles of Nuclear Magnetism*; Oxford University: London, 1961.

protons. The calculated second moments are 199 kHz² (11.0 Oe²) and 305 kHz² (16.8 Oe²) for the tetrahedral and the square planar configurations, respectively.¹⁸ The experimental second moment in a rigid lattice (202 kHz²) supports the tetrahedron model.

In the motional state, the second moment varies depending on the mode of the motion. If the translational motion were fast enough, M_2 should be zero. In the present case, the hydrogen motion is localized around nickel atoms, because the observed second moment (46.6 kHz²) is far from zero. If the NiH_4 unit undergoes an isotropic rotation, the dipolar interaction among the hydrogen atoms in the same unit is averaged out to zero, while the interunit interaction remains unaveraged. The interunit interaction can be estimated using eq 2, where the r_i value should be replaced by the distance between the centers of gravity of each unit. The calculated values are 42 kHz² (2.3 Oe²) and 40 kHz² (2.2 Oe²) for the tetrahedron and the square plane models, respectively.¹⁸ The experimental value (46.6 kHz²) can support both models. The small discrepancy might arise from the distortion of the tetrahedron and/or the inhomogeneous broadening caused by magnetic impurities such as Ni clusters on the particle surface.

The loss of the second moment due to the localized motion is 155 kHz². The corresponding values were obtained from the spin–lattice relaxation studies, which were 136 kHz² (7.5 Oe²) and 123 kHz² (6.8 Oe²) for ^1H $T_{1\rho}$ and T_1 , respectively.¹⁶ These values are in fair agreement with the present result. The small discrepancy suggests that the jump frequency has a distribution.

In conclusion, the ^1H results support the tetrahedral configuration as well as the isotropic rotation of the NiH_4 unit.

Conclusions

^2H and ^1H NMR spectra have been measured in the low-temperature phase of Mg_2NiD_4 and Mg_2NiH_4 , respectively. The results support the distorted tetrahedron model for the hydrogen distribution and the pseudoisotropic rotation of the tetrahedron as follows:

(1) The temperature dependence of ^2H NMR spectra is quite well simulated assuming the distorted tetrahedral configuration and the pseudoisotropic rotation. The jump frequency is estimated, which obeys Arrhenius relation with a frequency factor of $(0.8 \pm 0.6) \times 10^{13}$ Hz and an activation energy of 50.1 ± 1.4 kJ/mol.

(2) The observed ^1H second moments are 202 kHz² in the rigid lattice and 46.6 kHz² in a motional state. The value in the rigid lattice supports the tetrahedron model. The value in a motional state is explained by the isotropic rotation of the NiH_4 unit.

Acknowledgment. The authors are grateful to Dr. E. Akiba of our institute for the syntheses of Mg_2NiH_4 and Mg_2NiD_4 samples. They thank the late Prof. R. R. Vold for kindly providing the source program of MXET1 and Dr. M. Sugie of our institute for installing the program on the IBM SP2 system.

IC0106367